Mean-field study of Fe^{2+}- and Co^{2+}-doped diluted magnetic semiconductors

Y. H. Zheng and J. B. Xia
Chinese Center of Advanced Science and Technology (World Laboratory), P. O. Box 8730, Beijing 100080, China
and Institute of Semiconductors, Chinese Academy of Sciences, P. O. Box 912, Beijing 100083, China
(Received 28 January 2005; revised manuscript received 29 August 2005; published 14 November 2005)

Based on a modified mean-field model, we calculate the Curie temperatures of Fe^{2+}- and Co^{2+}-doped diluted magnetic semiconductors (DMSs) and their dependence on the hole concentration. We find that the Curie temperatures increase with an increase in hole concentration and the relationship $T_C \propto p^{1/3}$ also approximately holds for Fe^{2+}- and Co^{2+}-doped systems with moderate hole concentration. For either low or high hole concentrations, however, the $p^{1/3}$ law is violated due to the anomalous magnetization of the Fe^{2+} and Co^{2+} ions, and the nonparabolic nature of the hole bands. Further, the values of T_C for Fe^{2+}- and Co^{2+}-doped DMSs are significantly higher than those for Mn^{2+}-doped DMSs, due to the larger exchange interaction strength.

DOI: 10.1103/PhysRevB.72.195204 PACS number(s): 75.50.Pp, 75.10.Dg, 75.50.Gg

I. INTRODUCTION

The recent discovery of carrier-induced ferromagnetism in Mn-doped diluted magnetic semiconductors[1,2] (DMSs) has generated intense interest, due to its potential application in spintronic devices, which combine the functions of information processing and storage. Curie temperatures T_C in excess of 100 K have been realized in (Ga,Mn)As systems[3] by using low-temperature molecular beam epitaxy growth to suppress the surface segregation of Mn and formation of the MnAs second phase during growth. The origins of ferromagnetism in such Mn-doped DMSs have been investigated using a mean-field model,[4–7] in which the carrier polarization mediates a long-range ferromagnetic exchange between the Mn ions. This mean-field model was first proposed by Zener[8] and then extended by Dietl *et al.*[4] to study the Curie temperatures of Mn-doped DMSs. The calculated Curie temperatures for (Ga,Mn)As (Ref. 7) and *p*-(Zn,Mn)Te (Ref. 9) are in quantitative agreement with experiments.

In addition to Mn-based DMSs, semiconductors doped with 3*d* transition-metal atoms have also been investigated, and it was predicted from first-principles calculations that certain V-, Cr-, Fe-, Co-, or Ni-doped III-V and II-IV semiconductors exhibit ferromagnetism.[10,11] Experimentally, room-temperature ferromagnetism has been observed in (Ga,Cr)N,[12] (Al,Cr)N,[13] $(Ti,Co)O_2$,[14] and (Zn,V)O.[15] The origins of ferromagnetism in such systems, however, remain controversial. Recently, Blinowski *et al.*[16] discussed the position of electronic states introduced by transition-metal impurities in II-VI and III-V compounds and suggested that moderate concentration of delocalized holes might exist in some Fe- and Co-based III-V compounds. It is therefore very interesting to investigate the role of hole-mediated ferromagnetism in these systems.

The rest of the paper is organized as follows. In Sec. II, the mean-field model is outlined and is extended to account for Fe^{2+} and Co^{2+} ions. Numerical results and discussion are given in Sec. III, and a brief conclusion is given in Sec. IV.

II. THEORETICAL MODEL

The exchange interaction between a hole with spin $\vec{s}$ at position $\vec{r}$ and 3*d* transition-metal impurities[17] (e.g., Mn^{2+}, Fe^{2+}, Co^{2+}) is

$$H_{pd} = \beta \sum_I \vec{s} \cdot \vec{S}_I \delta(\vec{r} - \vec{R}_I), \tag{1}$$

where $\vec{S}_I$ is the spin of the magnetic ion at site I, and β is the *p-d* exchange integral. In the virtual-crystal and mean-field approximations, S_I is substituted with its thermally averaged value $\langle S_I \rangle$, and then Eq. (1) can be written as

$$H_{pd} = \beta \vec{s} \cdot \vec{M}/g\mu_B, \tag{2}$$

where $M = xN_0 g\mu_B S$ is the magnetization of the localized spins, x the concentration of the magnetic ions, N_0 the concentration of cation sites, g the Landé factor of the magnetic impurities, and S the spin angular momentum.

In the mean-field theory, the free energy functional of the electron and magnetic impurity system reads $F[M] = F_c[M] + F_S[M]$, where $F_c[M]$ and $F_S[M]$ are the free-energy functionals of the hole subsystems and localized spins, respectively. The hole free-energy functional $F_c[M]$ is obtained as follows. First we diagonalize the 6×6 Kohn-Luttinger Hamiltonian together with the *p-d* exchange interaction. Then we compute the partition function

$$Z = \mathrm{Tr}\, e^{-\beta(H_h - \varepsilon_F N)}, \tag{3}$$

where H_h is the hole Hamiltonian including the *p-d* exchange interaction in the mean field approximation, ε_F is the hole Fermi energy, and N is the number operator for holes. The hole free-energy is calculated from $F_c[M] = -k_B T \ln Z$. After some algebra, we obtain

$$F_c(p,M) = -k_B T \int d\varepsilon\, N(\varepsilon) \ln(1 + \exp\{-[\varepsilon(M) - \varepsilon_F(p,M)]/k_B T\}) + p\varepsilon_F(p,M), \tag{4}$$

where $N(\varepsilon)$ is the hole density of states. At low temperature, the hole liquid is degenerate, and

$$F_c(p,M) = \int_0^p dp'\, \varepsilon(M,p'). \tag{5}$$

Here, we use Gilat's method[18] to calculate the density of states and the free-energy functional $F_c(p,M)$.

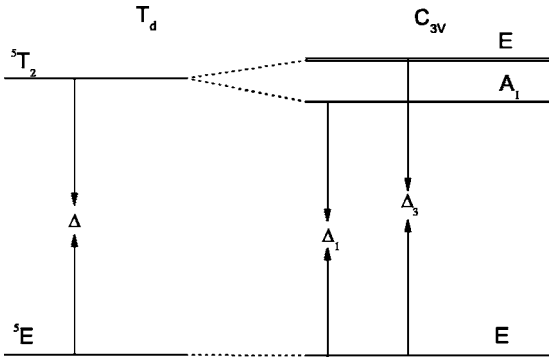

FIG. 1. Schematic diagram of the orbital energy levels of Fe^{2+} in T_d and C_{3v} crystal fields (Ref. 19).

The free-energy functional of the localized spins is given by

$$F_S[M] = \int_0^M dM_0 H(M_0), \tag{6}$$

where $M_0(H)$ is the magnetization of magnetic ions in an external magnetic field H in the absence of carriers. The Mn^{2+} ion has a ${}^6S_{5/2}$ ground state with negligible splitting in the crystal field, such that it behaves like a free ion. As a result, the magnetization of Mn^{2+} ions in DMSs, $M_0(H)$, can be described by the Brillouin function.[5,7] On the other hand, Fe^{2+} and Co^{2+} have D or F group terms which split in the tetrahedral or trigonal crystal field (cf. Figs. 1 and 2; see also the Appendix for details). Their magnetization in a magnetic field H can be obtained from

$$M_0(H) = xN_0 k_B T \frac{\partial}{\partial H} \ln Z, \tag{7}$$

where

$$Z = \sum_i \exp(-E_i/k_B T) \tag{8}$$

is the partition function of magnetic ions in the crystal field and external magnetic field. Because the crystal field induces level splitting, there are no analytical expressions for $M_0(H)$,

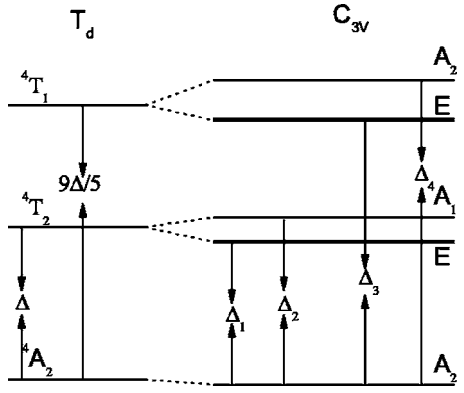

FIG. 2. Schematic diagram of the orbital energy levels of Co^{2+} in T_d and C_{3v} crystal fields (Ref. 19).

and it must be obtained numerically (see the Appendix for details).

By minimizing the total free-energy functional $F[M]$ with respect to M at a given temperature T and hole concentration p, in the absence of the external magnetic field, we obtain

$$H[M] = -\partial F_c[M]/\partial M. \tag{9}$$

This can be viewed as the effective magnetic field (produced by the hole subsystem) acting on the magnetic ions. It then produces a finite magnetization M of the magnetic ions according to Eq. (7). The equilibrium magnetization at a given temperature T and hole concentration p is obtained by solving Eqs. (7) and (9) self-consistently. The Curie temperature T_C is defined as the critical temperature at which the equilibrium magnetization M vanishes. When $T \to T_C$, we have $M \to 0$ and $H \to 0$. In this case, the dependence of magnetization on the effective magnetic field (produced by the hole subsystem) $M(H)$, in the form of Eq. (7), is reduced to

$$M = \chi_D H, \tag{10}$$

where

$$\chi_D = \left.\frac{\partial M}{\partial H}\right|_{H\to 0}, \tag{11}$$

is the differential susceptibility for the magnetic ions.

Combining Eqs. (9) and (10), we obtain the equation that determines the Curie temperature of a DMS, which reads

$$xN_0 k_B T \left.\frac{\partial^2 \ln Z}{\partial^2 H}\right|_{H\to 0} = \left.\frac{M^2}{2(F_c[p,0] - F_c[p,M])}\right|_{M\to 0}. \tag{12}$$

III. RESULT AND DISCUSSION

In this section, we calculate numerically the Curie temperatures of Fe^{2+}- and Co^{2+}-doped III-V and II-VI DMSs and discuss their dependence on hole concentration. We also compare the calculated Curie temperatures with those of Mn^{2+}-doped DMSs. The material parameters of zinc-blende semiconductors (ZnS, GaP, GaAs, ZnSe, InP, ZnTe, CdTe) are taken from Ref. 7, while those for the wurtzite semiconductor CdSe are taken from Ref. 20. The crystal field splitting and the spin-orbit coupling parameters for some Fe-doped zinc-blende DMSs are listed in Table I. Those for the wurtzite semiconductor CdSe are taken from Ref. 19: $\Delta_1 = 2800\ \mathrm{cm}^{-1}$, $\Delta_2 = 3300\ \mathrm{cm}^{-1}$, $\Delta_3 = 5200\ \mathrm{cm}^{-1}$, $\Delta_4 = 6000\ \mathrm{cm}^{-1}$, and $\lambda = -120\ \mathrm{cm}^{-1}$ for $Cd_{0.95}Co_{0.05}Se$; $\Delta_1 = 2592\ \mathrm{cm}^{-1}$, $\Delta_3 = 2724\ \mathrm{cm}^{-1}$, and $\lambda = -81\ \mathrm{cm}^{-1}$ for $Cd_{0.95}Fe_{0.05}Se$.

In Fig. 3, the paramagnetic susceptibilities χ_D of Mn^{2+}, Fe^{2+}, and Co^{2+} in a GaP crystal environment at vanishing external magnetic field ($H \to 0$) are plotted as functions of inverse temperature $1/T$. The susceptibility χ_D of Mn^{2+} ions shows a linear behavior with respect to $1/T$ over the whole temperature range, which comes from the Brillouin paramagnetism. For Co^{2+} and Fe^{2+} ions, however, the deviation becomes noticeable at low temperatures. For Fe^{2+} ions, χ_D

TABLE I. Parameters of some Fe^{2+}-doped compounds. The crystal parameters of ZnS, ZnTe, CdTe, and ZnSe are taken from Ref. 21, and those of GaAs, GaP, and InP from Refs. 22–24, respectively. The *p-d* exchange energy βN_0 of CdTe is taken from Ref. 25, the others from Ref. 17 or calculated by $\beta = \beta$ (ZnFeSe) (Ref. 7).

Material	ZnS	ZnTe	CdTe	ZnSe	GaAs	GaP	InP
Δ_c (cm^{-1})	3160	2690	2480	2930	3206	3559.4	3038
λ (cm^{-1})	−99	−96	−99	−85	−90.3	−93.5	−86.6
βN_0 (eV)	−2.01	−1.9	−1.27	−1.74	−1.76	−1.96	−1.57

even saturates at low enough temperatures. This peculiar behavior shows the Van Vleck paramagnetism of Fe^{2+}, since the lowest levels of Fe^{2+} ion split by the crystal field and the spin-orbit interaction are nondegenerate.[19] The deviation for Co^{2+} ions is smaller, for it has degenerate ground states and hence exhibits ordinary paramagnetism (see the Appendix for details). Further, it can be seen that the paramagnetic susceptibilities decrease in order of Mn^{2+}, Fe $^{2+}$, and Co^{2+} at high temperatures. This is because the magnetic moments of the iron group are mainly decided by their spin magnetic moments due to the orbital quenching,[26] and the spin magnetic moments decrease in order of Mn^{2+}, Fe^{2+}, and Co^{2+}. For simplicity, magnetic anisotropy is not discussed in this paper and χ_D is the susceptibility when H and M are parallel in the [001] crystal direction (other physical quantities are similar).

It is convenient to introduce an effective temperature-dependent spin angular momentum $S_{\text{eff}}(T)$, such that the paramagnetic susceptibilities $\chi_D(T)$ for other magnetic ions take the same form as that for Mn^{2+} ions:[7]

$$\chi_D = \frac{1}{3k_BT} S_{\text{eff}}(S_{\text{eff}}+1) x N_0 (g\mu_B)^2. \tag{13}$$

For Mn^{2+} ions, $S_{\text{eff}}=5/2$ is independent of temperature, while for Fe^{2+} and Co^{2+}, $S_{\text{eff}}(T)$ must be determined numerically from Eq. (11). For Fe^{2+} and Co^{2+} ions in a GaP (zinc-blende structure) or a CdSe (wurtzite structure) crystal environment, the effective spin angular momenta S_{eff} are plotted as functions of inverse temperature $1/T$ in the inset of Fig. 3. We see that the effective spin angular momenta S_{eff} are approximatively constant at high temperatures, while at low temperatures, they decrease with decreasing temperature. Now we can rewrite Eq. (12) in the form

$$T_C = -\frac{2}{3} S_{\text{eff}}(S_{\text{eff}}+1) x N_0 (g\mu_B)^2 \left. \frac{F_c[M]-F_c[0]}{k_B M^2} \right|_{M\to 0}. \tag{14}$$

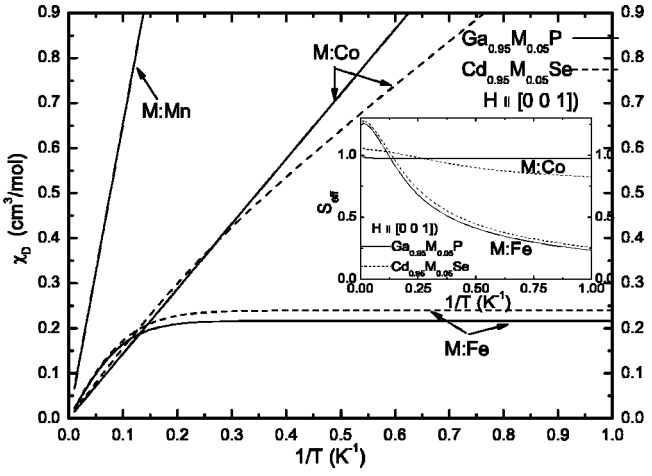

FIG. 3. Paramagnetic susceptibilities χ_D as functions of $1/T$ for Mn^{2+}, Fe^{2+}, and Co^{2+} in a GaP (zinc-blende structure) or a CdSe (wurtzite structure) crystal environment at $H\to 0$, crystal parameter of $Ga_{0.95}Co_{0.05}P$ is $\Delta=4750$ cm^{-1}, $\lambda=-134$ cm^{-1}. The insert figure shows the effective spin angular momenta of these DMSs as functions of $1/T$.

Generally, since S_{eff} is dependent on T, the equation has to be solved self-consistently. However, when the effective spin angular momentum of the magnetic ion S_{eff} is approximately independent of temperature, which is true for Co^{2+} and Fe^{2+} at high temperatures (see the inset of Fig. 3), Eq. (14) becomes an explicit expression for the Curie temperature [for Fe^{2+}-doped DMSs, it is only true at high hole concentration (corresponding to high Curie temperature)]. For a strongly degenerate hole liquid, and in the absence of spin-orbit interaction, we have $(F_c[M]-F_c[0])/M^2 \sim \beta^2 \rho_F$, where ρ_F is the density of states of holes on the Fermi surface.

From Eq. (14), it can be seen that the Curie temperature of DMSs in the mean-field model is mainly decided by three factors: (a) the density of states of the holes on the Fermi surface ρ_F, which is determined by the hole band structure of the host semiconductor; (b) the exchange energy $N_0\beta$ between the hole and the magnetic ions, where $N_0 \propto a^{-3}$ (a is the lattice constant of the host material), and β depends on the hybridization integral, the charge transfer energies between the hole band and the magnetic ions, and the magnitude of the local magnetic moment;[17] (c) the paramagnetic susceptibility χ_D [see Eq. (12)] or the effective spin angular momentum S_{eff} of the magnetic ions [see Eqs. (12) and (14)]. The first two factors, as well as the relationship $T_C \propto \beta^2$, have been discussed by Dietl *et al.* and Abolfath *et al.*[5,7] The approximate relationship $T_C \propto p^{1/3}$ was also discussed by Schliemann *et al.*[27] based on a simple parabolic band model. In the present work, we shall extend the relationship $T_C \propto p^{1/3}$ to multiband structures and non-Mn^{2+}-doped DMSs. We also discuss the effect of the last factor, i.e., the influence of the paramagnetic susceptibility χ_D. Though Eq. (14) is a self-consistent equation when S_{eff} is dependent on T, it is still easy to find that the Curie temperature decreases when S_{eff} becomes small, since S_{eff} decreases with decreasing temperature.

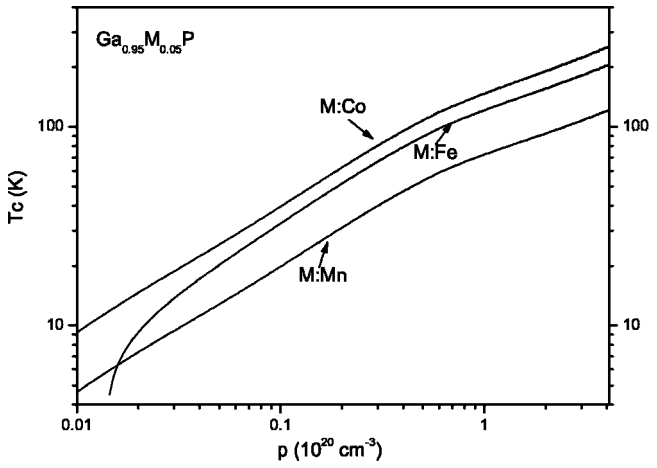

FIG. 4. Curie temperatures as functions of the hole concentration for zinc-blende structure $Ga_{0.95}M_{0.05}P$ with M=Co, Fe, and Mn, crystal parameter of $Ga_{0.95}Co_{0.05}P$ is Δ=4750 cm^{-1}, λ =−134 cm^{-1}.

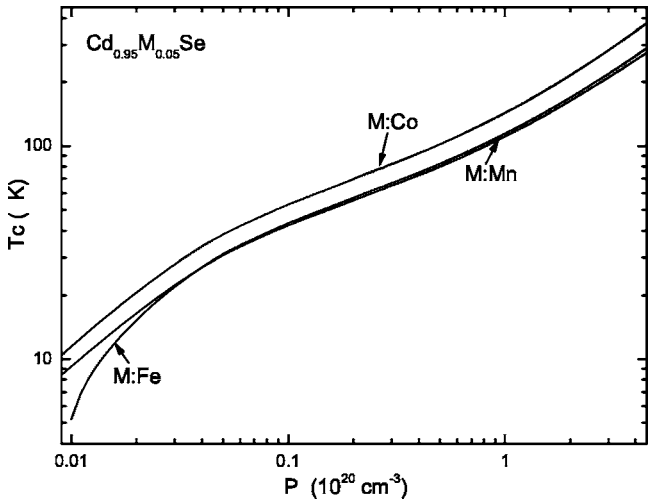

FIG. 5. Curie temperatures as functions of the hole concentration for wurtzite structure $Cd_{0.95}M_{0.05}Se$ with M=Co, Fe, and Mn.

In Fig. 4, the Curie temperatures as functions of hole concentration for $Ga_{0.95}M_{0.05}P$ (zinc-blende structure, M=Co, Fe, Mn) are presented. It can be seen that the Curie temperatures decrease in order of Co, Fe, Mn for a wide range of hole concentrations, while the Curie temperatures for Fe^{2+}- and Co^{2+}-doped DMSs cross at low enough hole concentrations. This behavior comes from the competition between the two factors (b) and (c) as follows. The local spin angular momenta for Co^{2+}, Fe^{2+}, and Mn^{2+} satisfy $S(Co^{2+}) < S(Fe^{2+}) < S(Mn^{2+})$. On the one hand, this leads to a similar relationship for the effective spin angular momenta, i.e., $S_{eff}(Co^{2+}) < S_{eff}(Fe^{2+}) < S_{eff}(Mn^{2+})$. On the other hand, the p-d exchange constants β for Co^{2+}, Fe^{2+}, and Mn^{2+} satisfy $\beta(Co^{2+}) > \beta(Fe^{2+}) > \beta(Mn^{2+})$, because β is inversely proportional to the local spin angular momentum.[17] The β factor dominates for most of the range of hole concentrations (e.g., the Curie temperature of $Ga_{0.95}Co_{0.05}P$ is about twice as high as that of $Ga_{0.95}Mn_{0.05}P$), since the difference between $S_{eff}(Co^{2+})$, $S_{eff}(Fe^{2+})$, and $S_{eff}(Mn^{2+})$ is small. For Fe^{2+}, the S_{eff} factor begins to dominate at small hole concentrations (or, equivalently, small Curie temperatures) since $S_{eff}(Fe^{2+})$ decreases rapidly with decreasing hole concentration. For a hole concentration $p < 1.5 \times 10^{18}$ cm^{-3}, $Ga_{0.95}Fe_{0.05}P$ becomes purely paramagnetic, due to the sufficiently small effective spin angular momentum $S_{eff}(Fe^{2+})$. Finally, we notice that the approximate relationship $T_C \propto p^{1/3}$ still holds for not-too-small hole concentrations, since the paramagnetic susceptibility χ_D is roughly proportional to $1/T$ (in the case that the effective spin angular momentum S_{eff} is independent of temperature), and at the same time, the density of states of holes on the Fermi surface ρ_F is roughly proportional to $p^{1/3}$. This behavior fails for Fe^{2+} at small hole concentrations because $\chi_D(Fe^{2+})$ approaches a constant value. Further, we can see that for high hole concentrations $p > 0.8 \times 10^{20}$ cm^{-3}, the relationship $T_C \propto p^{1/3}$ also fails, due to the effect of spin-orbit interaction.

In Fig. 5, we plot the Curie temperatures as functions of hole concentration for $Cd_{0.95}M_{0.05}Se$ (wurtzite structure, M=Co, Fe, and Mn). We see that the Curie temperatures show similar behaviors as in Fig. 4. As we have discussed previously, the behavior of the Curie temperature as a function of hole concentration is primarily determined by the p-d exchange constants β, the effective spin angular momentum S_{eff}, and the density of states ρ_F on the Fermi surface. The similar relationship $\rho_F \propto p^{1/3}$ and the similar behavior of β and $S_{eff}(T)$ in wurtzite semiconductors lead to similar dependence of the Curie temperature on the hole concentration.

From the above discussions, we see that Curie temperatures for Fe^{2+}-doped DMSs are quite different from those for Mn^{2+} ones. Therefore, we show Curie temperatures of some Fe^{2+}-doped III-V and II-VI DMSs (zinc-blende structure) in Fig. 6. We can find a similar chemical trend to those of Mn^{2+}-doped DMSs. That is, the Curie temperatures increase with decreasing spin-orbit splitting [which enhances the

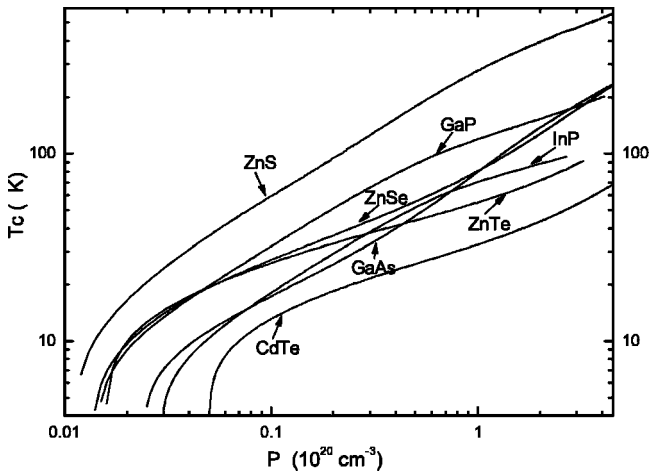

FIG. 6. Curie temperatures as functions of the hole concentration for some semiconductors doped with 5% of Fe^{2+}.

density of states ρ_F on the Fermi surface as in Eq. (14)], decreasing lattice constant of the host semiconductor, increasing *p-d* exchange energy, and increasing hole effective mass (which also leads to an increase of ρ_F). It can be seen in Fig. 6 that $Zn_{0.95}Fe_{0.05}S$ has the highest Curie temperature, because of its small lattice constant and large hole effective mass. Again, the relationship $T_C \propto p^{1/3}$ fails at either high or low hole concentrations. The failure at small hole concentrations comes from the failure of the relationship $\chi_D \propto 1/T$ at low temperatures, while the failure at high hole concentrations comes from the influence of spin-orbit split-off bands. Therefore, the relationship $T_C \propto p^{1/3}$ breaks down due to the deviation of χ_D from the $1/T$ law for non-Mn^{2+}-doped DMSs. Even for Mn^{2+}-based DMSs, it is also modified by the spin-orbit interaction and nonparabolic band structure. Therefore, it is very important to take into account both the $\mathbf{k}\cdot\mathbf{p}$ interaction and spin-orbit splitting in the host semiconductor in real Curie temperature calculations.

IV. CONCLUSIONS

Based on a modified mean-field model, we calculate the Curie temperatures of Fe^{2+}- and Co^{2+}-doped DMSs and their dependence on the hole concentration. We find that the Curie temperatures increase with an increase of hole concentration and the relationship $T_C \propto p^{1/3}$ also approximately holds for Fe^{2+}- and Co^{2+}-doped DMSs for moderate hole concentrations. For either low or high hole concentrations, however, the $p^{1/3}$ law is violated due to the anomalous magnetization of Fe^{2+} and Co^{2+} ions and the nonparabolic nature of the hole bands. Further, the values of T_C of Fe^{2+}- and Co^{2+}-doped DMSs are significantly higher than those of Mn-doped DMSs due to the larger exchange interaction strength.

ACKNOWLEDGMENTS

This work was supported by the National Natural Science Foundation Grant No. 90301007, and the special funds for Major State Basic Research Project No. G001CB3095 of China.

APPENDIX

In the DMSs, the magnetic ion is surrounded by other ions, giving rise to an electrostatic potential called the crystalline potential (or crystal potential). Thus, without including the influence of carriers, the total Hamiltonian of the magnetic ion in order of decreasing magnitude is

$$H = H_0 + V_C + \lambda \vec{L}\cdot\vec{S} + \mu_B \vec{B}\cdot(\vec{L}+2\vec{S}), \tag{A1}$$

where H_0 is the free-ion Hamiltonian excluding of spin-orbit interactions, V_C is the crystalline potential, the third term is the spin-orbit coupling term (L and S are orbital and spin angular momentum), and the last term is the Zeeman interaction where we approximate the electron g-factor, $g_s \approx 2$. Here we use the method of operator equivalents introduced by Stevens[19,28] to solve the crystal potential problem. As described in Ref. 19, the crystal potential in a cubic environment can be written in the form

$$V_c = V_c(T_d) + V_c(C_{3v}) \tag{A2}$$

$$\begin{aligned} &= \left(\frac{c-2a}{60}\right)[35L_\zeta^4 - 30L(L+1)L_\zeta^2 \\ &\quad + 25L_\zeta^2 - 6L(L+1) + 3L^2(L+1)^2] \\ &\quad - \left(a\frac{\sqrt{2}}{6}\right)\{L_+^3 + L_-^3, L_\zeta\} \\ &\quad + b\left(\frac{L(L+1)}{3} - L_\zeta^2\right), \end{aligned} \tag{A3}$$

where

$$L_\pm = L_\xi \pm iL_\eta, \tag{A4}$$

$$\{u,v\} = uv + vu, \tag{A5}$$

and a, b, and c are constants, ξ, η, and ζ are coordinate axes with ζ along [1 1 1].[19] To describe the energy levels of transition ions in the site of symmetry T_d or C_{3v}, we use the representation in which L_ζ is diagonal, i.e.,

$$L_\zeta \phi_\mu = \mu\phi_\mu, \tag{A6}$$

$\mu = L, L-1, \ldots, -(L-1), -L$.

Then we can exactly diagonalize the $(2L+1)\times(2L+1)$ matrix whose elements are $\langle\phi_{\mu'}|V_c|\phi_\nu\rangle$. We denote the ground state by $|0\rangle$ and choose its energy as 0. Then the excited states and corresponding energy levels are denoted by $|1\rangle, |2\rangle, \ldots, |n\rangle$ and $\Delta_i\,(i=1,2,3,\ldots)$, respectively. Of course, the ground state and excited states may be further split when considering

$$H' = \lambda\vec{L}\cdot\vec{S} + \mu_B\vec{B}\cdot(\vec{L}+2\vec{S}). \tag{A7}$$

To the second order, the matrix elements of the Hamiltonian H' for the ground state are

$$\begin{aligned} \langle 0_j, M_s'|H'|0_i, M_s\rangle &= \langle 0_j, M_s'|H'|0_i, M_s\rangle \\ &\quad - \sum_{n_k}\sum_{M_s''}\sum_k \Delta_n^{-1}\langle 0_j, M_s'|H'|n_k, M_s''\rangle \\ &\quad \times\langle n_k, M_s''|H'|0_i, M_s\rangle, \end{aligned} \tag{A8}$$

where the subscripts j,k in $|0_j\rangle, |n_k\rangle$ are used to distinguish degenerate states.

Now we analyze the energy levels of Fe^{2+} and Co^{2+} in a cubic environment. The electronic configuration of Fe^{2+} is $(3d)$,[6] and according to Hund's rules, the ground state of the free ion is $^5D_4$. The fivefold orbital degeneracy of Fe^{2+} first splits into an orbital triplet $T_2(T_d)$ and a lower orbital doublet $E(T_d)$ under the crystal field of T_d symmetry (Fig. 1) (the analysis of the C_{3v} symmetry crystal field is similar). The tenfold $E(T_d)$ and 15-fold $T_2(T_d)$ are further split by the spin-orbit interaction. Thus, since the lowest energy level is nondegenerate, Fe^{2+} in the crystalline environment will only show Van Vleck paramagnetism at low temperatures. The electronic configuration of Co^{2+} is $(3d)$,[7] and the ground

state of the free ion is $^4F_{9/2}$. In a crystal of T_d symmetry, the sevenfold orbital degeneracy of Co^{2+} splits into an $A_2(T_d)$ singlet and $T_2(T_d)$ and $T_1(T_d)$ triplets (Fig. 2). For large crystal field splitting, we need only consider the split of the tenfold $E(T_d)$ for Fe^{2+} and the fourfold $A_2(T_d)$ for Co^{2+} by the spin-orbit coupling and the Zeeman interaction.

[1] H. Ohno, H. Munekata, T. Penney, S. von Molnar, and L. L. Chang, Phys. Rev. Lett. **68**, 2664 (1992).

[2] H. Ohno, A. Shen, F. Matsukara, A. Oiwa, A. Endo, S. Katsumoto, and Y. Iye, Appl. Phys. Lett. **69**, 363 (1996).

[3] F. Matsukura, H. Ohno, A. Shen, and Y. Sugawara, Phys. Rev. B **57**, R2037 (1998).

[4] T. Dietl, H. Ohno, F. Matsukura, J. Cibert, and D. Ferrand, Science **287**, 1019 (2000).

[5] M. Abolfath, T. Jungwirth, J. Brum, and A. H. MacDonald, Phys. Rev. B **63**, 054418 (2001).

[6] D. J. Priour, Jr., E. H. Hwang, and S. Das Sarma, Phys. Rev. Lett. **92**, 117201 (2004).

[7] T. Dietl, H. Ohno, and F. Matsukura, Phys. Rev. B **63**, 195205 (2001).

[8] C. Zener, Phys. Rev. **81**, 440 (1950); **83**, 299 (1951).

[9] D. Ferrand, J. Cibert, A. Wasiela, C. Bourgognon, S. Tatarenko, G. Fishman, T. Andrearczyk, J. Jaroszynski, S. Kolesnik, T. Dietl, B. Barbara, and D. Dufeu, Phys. Rev. B **63**, 085201 (2001).

[10] K. Sato and H. Katayama-Yoshida, Jpn. J. Appl. Phys., Part 2 **39**, L555 (2000).

[11] K. Sato and H. Katayama-Yoshida, Semicond. Sci. Technol. **17**, 367 (2002).

[12] S. E. Park, H. J. Lee, Y. C. Cho, S. Y. Jeong, C. R. Cho, and S. Cho, Appl. Phys. Lett. **80**, 4187 (2002).

[13] D. Kumar, J. Antifakos, M. G. Blamire, and Z. H. Barber, Appl. Phys. Lett. **84**, 5004 (2004).

[14] Y. Matsumoto, M. Murakami, T. Shono, T. Hasegawa, T. Fukumura, M. Kawasaki, P. Ahmet, T. Chikyow, S. Koshihara, and H. Koinuma, Science **291**, 854 (2001).

[15] H. Saeki, H. Tabata, and T. Kawai, Solid State Commun. **120**, 439 (2001).

[16] J. Blinowski, P. Kacman, and T. Dietl, in *Materials Research Society Symposia Proceedings* No. 690, edited by T. J. Klemmer, J. Z. Sun, A. Fert (Materials Research Society, Pittsburgh, 2002).

[17] P. Kacman, Semicond. Sci. Technol. **16**, R25 (2001).

[18] G. Gilat and L. J. Ranbenheimer, Phys. Rev. **144**, 390 (1966).

[19] M. Vlleret, S. Rodriguez, and E. Kartheuser, Physica B **162**, 89 (1990).

[20] J. B. Xia and J. Li, Phys. Rev. B **60**, 11540 (1999).

[21] J. P. Mahoney, C. C. Lin, W. H. Brumage, and F. Dorman, J. Chem. Phys. **53**, 4286 (1970).

[22] K. Pressel, G. Rückert, A. Dörnen, and K. Thonke, Phys. Rev. B **46**, 13171 (1992).

[23] C. L. West, W. Hayes, J. F. Ryan, and P. J. Dean, J. Phys. C **13**, 5631 (1980).

[24] K. Pressel, K. Thonke, A. Dörnen, and G. Pensl, Phys. Rev. B **43**, 2239 (1991).

[25] C. Testelin, C. Rigaux, A. Mycielsi, and M. Menant, Solid State Commun. **78**, 659 (1991).

[26] C. Kittel, *Introducton to Solid State Physics*, 7th ed. (J. Wiley and Sons, New York, 1996), p. 426.

[27] J. König, J. Schliemann, T. Jungwirth, A. H. MacDonald, in *Electronic Structure and Magnetism of Complex Materials*, edited by D. J. Singh and D. A. Papaconstantopoulos (Springer-Verlag, Berlin, 2002).

[28] K. W. H. Stevens, Proc. Phys. Soc. London **65**, 209 (1952).